International Journal of Mechanical, Industrial and Aerospace Sciences
ISSN: 2517-9950
Vol:7, No:7, 2013

Robotic End-Effector Impedance Control without Expensive Torque/Force Sensor

Shiuh-Jer Huang, Yu-Chi Liu, and Su-Hai Hsiang

***Abstract*—**A novel low-cost impedance control structure is proposed for monitoring the contact force between end-effector and environment without installing an expensive force/torque sensor. Theoretically, the end-effector contact force can be estimated from the superposition of each joint control torque. There have a nonlinear matrix mapping function between each joint motor control input and end-effector actuating force/torques vector. This new force control structure can be implemented based on this estimated mapping matrix. First, the robot end-effector is manipulated to specified positions, then the force controller is actuated based on the hall sensor current feedback of each joint motor. The model-free fuzzy sliding mode control (FSMC) strategy is employed to design the position and force controllers, respectively. All the hardware circuits and software control programs are designed on an Altera Nios II embedded development kit to constitute an embedded system structure for a retrofitted Mitsubishi 5 DOF robot. Experimental results show that PI and FSMC force control algorithms can achieve reasonable contact force monitoring objective based on this hardware control structure.

***Keywords*—**Robot, impedance control, fuzzy sliding mode control, contact force estimator.

I. Introduction

ROBOTIC manipulator had been widely used in industrial automation applications owing to its quickly operation speed and accurate position control features. The end-effector grasping/contact force monitoring ability is an important factor for obtaining robotic compliance to execute further intelligent grinding, assembly and human-interaction applications. However, the force control for achieving desired robotic compliance has been known to be a complicated control problem. There had several control approaches for establishing robotic compliance. Hogan [1] proposed an impedance force-control concept with a 2nd order differential equation to described the relationship between contact force and end-effector working position. Based on external dynamics behavior to determine the contact force between end-effector and environment, the position control was used to monitor the end-effector contact force by using appropriate position command. The same controller was designed in spite of end-effector contacted with environment or not. However, the complete dynamic model of a robot is not known exactly, and the environment stiffness is also estimated roughly. The control performance of this contact force monitoring scheme will degrade with respect to the system dynamic model error. Jung and Hsia [2] used a neural network algorithm to compensate the manipulator dynamic model uncertainty for improving the impedance control robustness. The impedance force tracking control strategy was proposed [3], too.

Hybrid motion control is another approach proposed by Mason [4] and Raibert and Carig [5]. The force and position are monitored separately based on the environmental constraint of motion trajectory. The contact stability problem of this model-based force control system was proved [6]. Ferretti et al. [7], [8] proposed a triangular control scheme to monitor the contact forces in the constrained directions without disturbing motion planning manipulated by the position control system. Force control is implemented as an outer loop, closed around the decentralized position control loops. The dynamics of the environmental constraint direction was considered for designing position control to obtain the force control demand without a switch between position and force control strategy.

For the impedance or hybrid position/force control, an expensive force/torque sensor is required for force measurement. It hinders the industrial applications. Mills and Goldenberg [9] employed a model-based constraint dynamics equation to calculate the contact force in constraint direction by using Lagrange Multiplier. This is an indirect force control scheme by using position controller worked on un-constrained direction without force sensor feedback. However, the control performance of this approach is limited to the dynamics model accuracy and robot degree of freedom (DOF). Here, a hybrid position/force control structure was established for a retrofitted Mitsubishi 5 DOF robot without the requirement of expensive force/torque sensor. The hall sensor is installed into each servo motor driver circuit for measuring its actuating current. Based on the specific relationship between each motor driver current and output torque, each motor instantaneous output torque can be calculated. Both control components of each joint position and force control schemes can be separately calculated at certain specific Cartesian positions for hybrid control purpose. The relationship function between the end-effector contact force with environment and each motor current input increment can also be established based on experimental tests. This function can be pre-found based on an installed force/torque sensor experimental data and curve fitting scheme for off-line calibration. Then this function can be employed in on-line contact force estimation and hybrid force control component calculation.

The proposed robotic hybrid impedance controller without force sensor installation has model free intelligent feature and it is robust with respect to uncertainties of robot dynamic model. The main idea is to design a simple fuzzy sliding mode

Shiuh-Jer Huang, Yu-Chi Liu, and Su-Hai Hsiang are with the Department of Mechanical Engineering, National Taiwan University of Science and Technology, 106, Keelung Road, Sec. 4, Taipei, Taiwan. (e-mail: {sjhuang, m1003435, shhsiang} @mail.ntust.edu.tw).

controller for each joint for minimizing the position tracking error directly and manipulating the robot tracking a desired trajectory to a specific position first. Then multi fuzzy sliding mode controllers are designed for minimizing the force tracking error. Both control laws are added together to constitute a hybrid controller for a 5 DOF Mitsubishi robot. Experimental results of specific contact force and force trajectory tracking control cases at certain position are presented to evaluate the performance of the proposed control scheme.

II. Control System Structure

The retrofitted robotic control structure of a 5 DOF Mitsubishi robot RV-M2 with Atera Nios II embedded development kit is shown in Fig. 1. The motors encoder resolutions are 740, 970, 740, 630, and 460 pulses per degree for joint 1 to joint 5, respectively. This Nios II development board has an embedded Atera Stratix system-on-a-programmable-chip (SOPC). It is employed to send DC servo motor digital control signals for actuating each joint motor of the robotic system; and detect each joint motor encoder position feedback. Here, Verilog HDL (Hardware Description Language) is selected to code the hardware circuits of this robotic servo control system for constituting a FPGA control system. The main functions of FPGA hardware circuits are motor optical encoder decoding, limit switch detecting, pulse width modulation (PWM) generating and hall sensors reading. The functions of the Nios II micro-processor software programs are the communication with PC by using UART, robotic inverse kinematics calculation, robotic motion trajectory planning, and robotic motion control schemes. A 13 bits control signal is used to regulate the duty circle of the servo motor PWM signal.

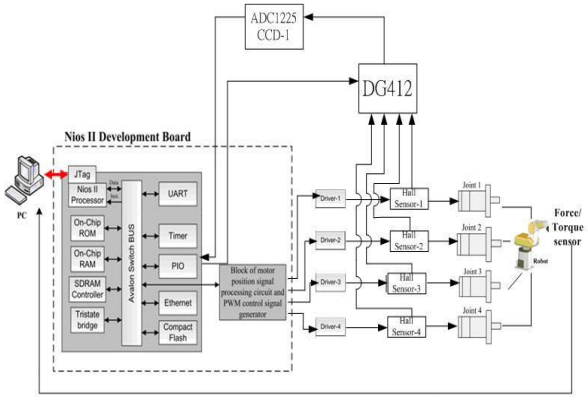

Fig. 1 Robotic force control system structure

The torque-force sensor used in this study for calibration purpose is a 6 axes force sensor FT8159 of ATI company with measuring ranges Fz=100N, Fx=Fy=32N, Tx=Ty=Tz=2.5N-m. It can be installed in the end-effector of this Mitsubishi robot. LEM company hall sensor HX-05P is used to measure each servo motor driving current and convert into digital signal before sent back to FPGA chip by an A/D IC.

III. Robot Inverse Kinematics

In order to achieve the manipulator positioning and trajectory tracking control purpose in workspace, the kinematics and inverse kinematics and trajectory planning should be investigated. Generally, the end-effector working position or motion path in Cartesian space are converted into control variables in joint coordinates for controlling purpose by using the inverse kinematics and Denavit-Hartenberg transformation matrix. Although some efficient analysis methods had been proposed [10], [11], they are time consuming and complicated mathematical operations. Since most of the assembly or pick-and-place operations are planned on a horizontal plane in working space, the end-effector orientation is specified as orthogonal and point down to the X-Y horizontal plane. Then the Denavit-Hartenberg transformation matrix of end-effector with respect to the reference inertia coordinate is

$$ {}^{ref}T_{tool} = {}^{0}A_1 \cdot {}^{1}A_2 \cdot {}^{2}A_3 \cdot {}^{3}A_4 \cdot {}^{4}A_5 = \begin{bmatrix} 1 & 0 & 0 & x \\ 0 & -1 & 0 & y \\ 0 & 0 & -1 & z \\ 0 & 0 & 0 & 1 \end{bmatrix} \quad (1) $$

Based on the Mitsubishi Movemaster RV-M2 robot link parameters, Table I, and forward kinematics calculation, the Denavit-Hartenberg transformation matrix can be derived and described by using the robotic D-H parameters a_i and θ_i. The joint angle θ_i can be solved by comparing the D-H matrix components and some trigonometric functions operations based on following steps:

Step 1: $\theta_1 = \theta_5 = A\tan 2(p_y, p_x)$

Step 2: $b = \pm\sqrt{(x^2 + y^2)}$

Step 3: $$\theta_3 = \cos^{-1}\left(\frac{b^2 + (d_1 - d_5 - z)^2 - a_1^2 - a_1(b - a_1) - a_2^2 - a_3^2}{2a_2a_3}\right) \quad (2)$$

Step 4: $$\theta_2 = A\tan 2\frac{(a_2 + a_3C_3)(d_1 - d_5 - z) - (a_3S_3)\cdot b}{(a_2 + a_3C_3)\cdot b + a_3S_3\cdot(d_1 - d_5 - z)}$$

Step 5: $\theta_4 = -\theta_2 - \theta_3$

This approach can reduce the trigonometric functions calculation from 17 times to 7 comparing with that of traditional inverse kinematics. The computer time on the Nios II SOPC can be reduced from 4.5ms to 2.5ms for increasing the system closed loop frequency.

IV. Mapping Function Between Joint Motors Control Input and End-Effector Contact Force

Since, the contact force between end-effector and environment will be monitored based on the hall senor current feedback only without torque/force sensor, the linearized functional mapping between each servo motor current input increment and the contact force components increment at certain specified working positions should be established first. The control performance is sensitive to this incremental

mapping function and the hall sensor current feedback. Hence, the hall sensor linearity evaluation, force sensor calibration and digital filter design should be executed before the mapping function searching experiments. The relationship between the hall sensor input current and output voltage is plotted in Fig. 2. It can be observed that there has a good linearity with a convert constant 1.25. In addition, the four-bit delay filter with 400 K Hz input frequency is employed to suppress the noise signal of encoders, limit switch and A/D IC output.

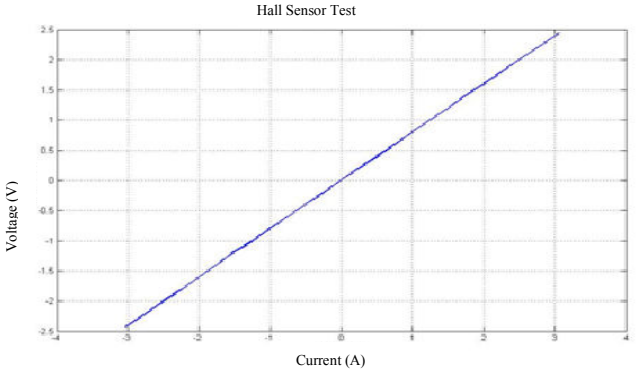

Fig. 2 Relationship between hall sensor current input and voltage output

The calibration of ATI torque/force sensor FT8159 was done by using standard 1 Kg weight on gravity field. Based on the force sensor output components in X, Y and Z direction, the calibration slope factor can be found as 8.8, 8.9 and 9.07, respectively. Then the accurate contact force can be calculated as:

$$F_{i\_real} = F_{i\_sensor} \frac{9.80665}{slope_i} \quad (3)$$

Since the hall sensor current feedback is adopted instead of force sensor for this robotic force control structure, the end-effector contact force is estimated based on joints motors current input increment and a mapping function matrix between force components and joints input current. This function is dependent on Cartesian space positions. Hence, three end-effector working positions are specified for establishing the contact force mapping function matrices. They can only be used for certain specified points with position and force separate control status. It is usefully for general assembly, grinding and man-machine interactive operations.

Robot is manipulated to a specified Cartesian point based on position control loop first. Then the closed loop control is switched off and the holding in-position control input of each joint motor is set as the reference. Thereafter, servo motors control input PWM value were changed once per joint and the corresponding current increment, ΔI, and three force sensor measuring component increment, ΔF were recorded. Here, joint 5 for end-effector self-rotation is fixed. Then the following experimental data relationship is obtained.

$$\begin{pmatrix} \Delta F_x \\ \Delta F_y \\ \Delta F_z \end{pmatrix} = \begin{bmatrix} a_1 & a_2 & a_3 & a_4 \\ b_1 & b_2 & b_3 & b_4 \\ c_1 & c_2 & c_3 & c_4 \end{bmatrix} \begin{bmatrix} \Delta I_1 \\ \Delta I_2 \\ \Delta I_3 \\ \Delta I_4 \end{bmatrix} \quad (4)$$

Although, these constant matrix coefficients can be estimated approximately based on multi experimental data sets and least square scheme, the force control purpose cannot be achieved appropriately by using the obtained constant matrix. The control force is diverged frequently during experimental test runs. The reason is that the optimal approximate solution of least square scheme may not satisfy this control system hardware constraint conditions and the transformation between each joint motor input current and force component increment is not a constant gain. Actually, their relationship is a nonlinear function mapping. Hence, multi-order polynomial function is chosen for simulating the individually relationship mapping of each matrix component a_{ij} . Here, curve fitting scheme is employed to establish the mapping function of each transfer matrix component.

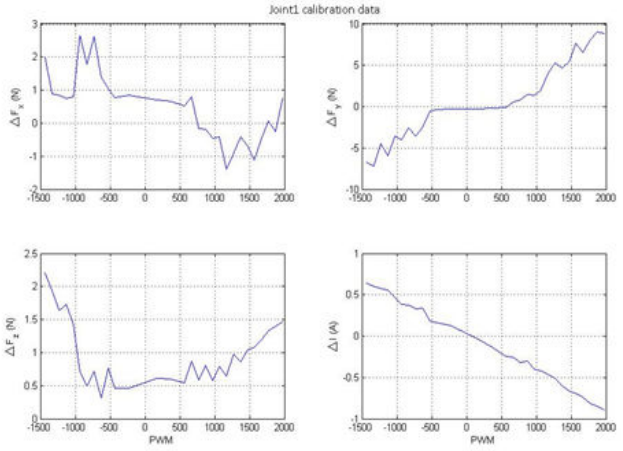

Fig. 3 Joint 1 current increment and end-effector contact force variation

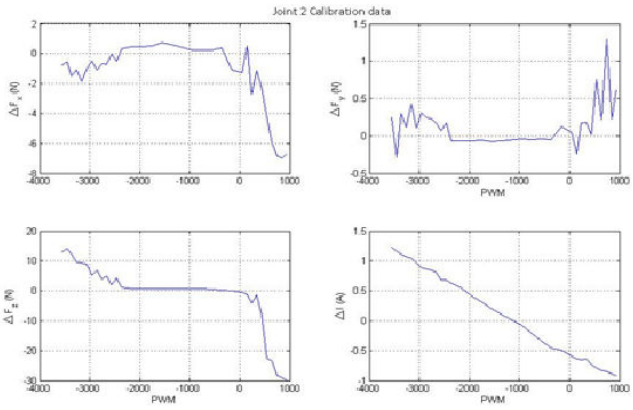

Fig. 4 Joint 2 current increment and end-effector contact force variation

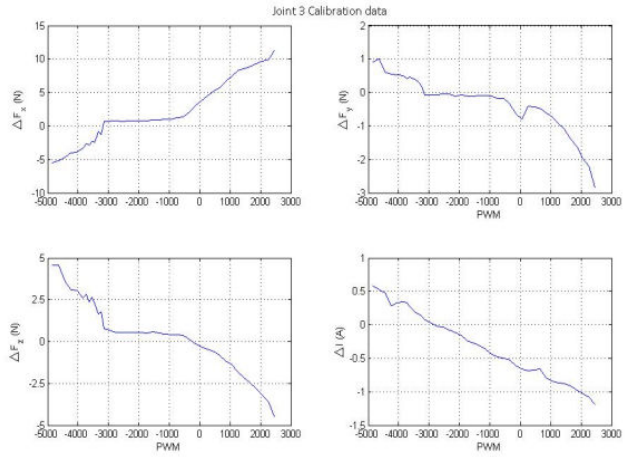

Fig. 5 Joint 3 current increment and end-effector contact force variation

Firstly, enough number of the open loop control current input increment and contact force components increment experimental data sets were obtained and plotted in Figs. 3-5. The working position is (450, 0, 145)mm in Cartesian space and the joint servo motor control input is PWM value. The corresponding hall sensor current increment and each force components increment curves are plotted. It can be observed that the hall sensor current feedback signal has an approximate linear relationship with respect to the PWM input. Hence, we can adjust the motor PWM input value to indirectly control the contact force variation. Since those relations are not linear, multi-order polynomial cure fitting scheme was employed to establish those functional mapping by using MATLAB polyfit and polyval toolbox. Although, higher order polynomial has better approximation accuracy, it needs more operation time on NIOS II developing board during real-time application. Here 3rd order polynomial was adopted to simulate those mapping function matrix components. The comparison of experimental data and 3rd order fitting curve are plotted in Figs. 6-8 for comparison. The coefficients of those polynomials are list in Table I for joint 1-3.

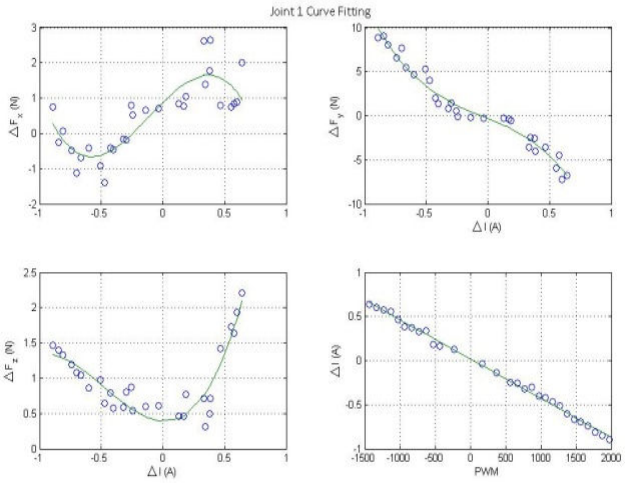

Fig. 6 Joint 1 3rd functional mapping between current increment and contact force

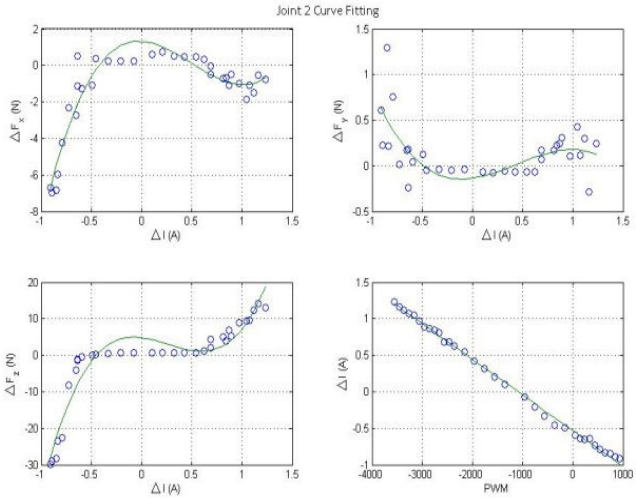

Fig. 7 Joint 2 3rd functional mapping between current increment and contact force

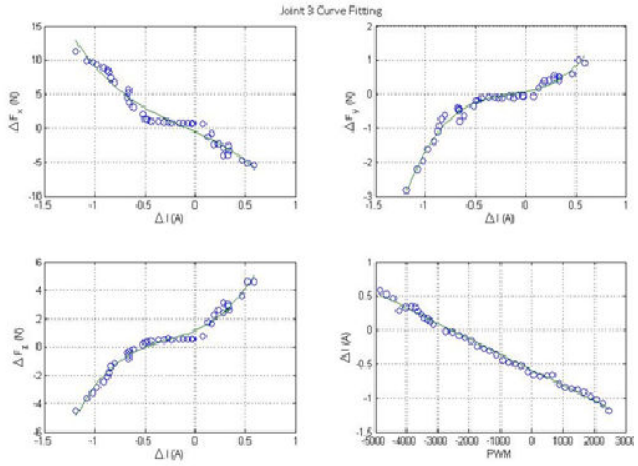

Fig. 8 Joint 3 3rd functional mapping between current increment and contact force

V. Fuzzy Sliding Mode Control

Since, the multi degree of freedom robotic control system has nonlinear and complicated dynamics behavior; it is difficult to establish an appropriate dynamic model for the model based controller design, especially for the onboard microprocessor. Here, the hybrid position/force switching control system has complicated dynamics behavior, an efficient and robustness controller must be designed to monitor the working position and force separated simultaneously. Here the sliding mode concept [12] is combined with fuzzy control strategy to design a model-free fuzzy sliding mode controller (FSMC) for robotic motion control. The fuzzy sliding control block diagram for hybrid position and force control is shown in Fig. 9 (a). It is an enhanced and extended development from the original FSMC approach proposed by Huang and Lin [13] to achieve excellent performance.

A sliding surface on the phase plane can be defined as

$$s(t) = (\frac{d}{dt} + \lambda)e_1 = e_2 + \lambda e_1 \quad (5)$$

where $e_i = x_{id} - x_i$ are defined as the state control errors. This sliding variable, s, was used as the input signal for establishing a fuzzy logic control system to approximate the specified perfect control law, u_{eq}. With this perfect control law, the closed loop control system has an asymptotical stability dynamic behavior [13].

$$\dot{s}(t) + \lambda s(t) = 0 \quad (6)$$

Here, a model-free fuzzy system was employed to substitute the mapping between the sliding variable, s, and the control law, u. This control law may have certain difference with the perfect control law u_{eq}, then the simplified sliding surface dynamics equation can be derived as.

$$\dot{s}(t) = -\lambda s(t) + b(X,t)[u_{eq}(t) - u(t)] \quad (7)$$

Generally, $b(X)$ is a positive constant or a positive slow time-varying function for practical physical systems. By multiplying both sides of the above equation with s gives

$$s(t)\dot{s}(t) = s(t)\{-\lambda s(t) + b(X,t)[u_{eq}(t) - u(t)]\} \quad (8)$$

Based on the Lyapunov theorem, the sliding surface reaching condition is $s \cdot \dot{s} < 0$. If a control input u can be chosen to satisfy this reaching condition, the control system will converge to origin of the phase plane. It can also be found that $\dot{s}$ increases as u decreases and vice versa in (7). If $s > 0$, then the increasing of u will result in $s\dot{s}$ decreasing. When the condition is $s < 0$, $s\dot{s}$ will decrease with the decreasing of u. Based on this qualitative analysis, the control input u can be designed with an attempt to satisfy the inequality $s \cdot \dot{s} < 0$. The relating theory about the convergence and stability of the adaptation process on the basis of the minimization of $s\dot{s}$ can be found in [14].

Here, a fuzzy logic control is employed to approximate the nonlinear function of equivalent control law, u_{eq}. The control input change for each sampling step is derived from fuzzy inference and defuzzification calculation instead of the equivalent control law derived from the nominal model at the sliding surface. It can eliminate the chattering phenomenon of a traditional sliding mode control. The controller design does not need a mathematical model and without constant gain limitation. The one dimensional fuzzy rules, Fig, 9 (b), is designed based on the sliding surface reaching condition, $s \cdot \dot{s} < 0$.

Here, eleven fuzzy rules are employed in this control system to obtain appropriate dynamic response and control accuracy. The input membership functions are scaled into the range of -1 and +1 with equal span. Hence a scaling factor gs is employed to map the sliding surface variable, s, into this universe of discourse. A scaling factor gu is employed to adjust the value of servo motor PWM control value.

The membership function used for the fuzzification is of a triangular type. The function can be expressed as

$$\mu(x) = \frac{1}{w}(-|x - a| + w) \quad (9)$$

where w is the distribution span of the membership function, x is the fuzzy input variable and a is the parameter corresponding to the value 1 of the membership function. The height method is employed to defuzzify the fuzzy output variable for obtaining the control PWM value of each joint control motor. Which is a nonlinear function derived from the fuzzy inference decision and defuzzification operation.

$$u = \frac{\sum_{l}^{m} \mu^{j} \cdot U^{j}}{\sum_{l}^{m} \mu^{j}} = \frac{\sum_{l}^{m} \mu^{j} \cdot C^{j}}{\sum_{l}^{m} \mu^{j}} \equiv \sum_{1}^{m} \phi_{j} C^{j} \quad (10)$$

where m is the rules number and C^j is the consequent parameter. Here, eleven equal-span triangular membership functions are used for the fuzzy input variable, s, and the fuzzy output variable, u.

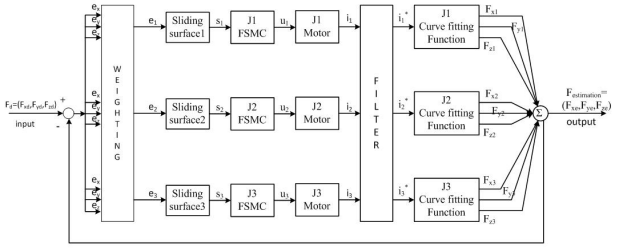

(a)

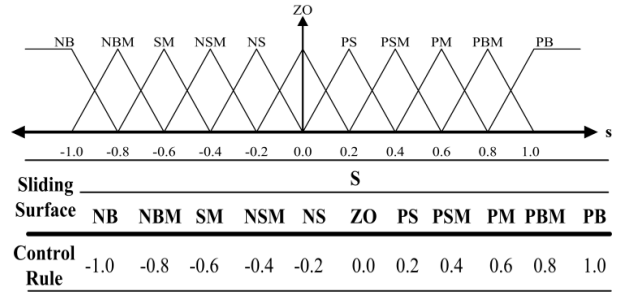

(b)

Fig. 9 (a) Fuzzy sliding mode contact force control block diagram, and (b) fuzzy membership functions and fuzzy control rules

When a robot is moving in un-constraint working space or holding at a specified position, each joint motor of this robot needs to provide certain torque for sustaining the weight of robot arm and executing the acceleration or deceleration operation. This sustaining component calculated from the position controller should be considered and introduced into the force or impedance controller for obtaining robotic end-effector compliance. In this study, the desired end-effector force or impedance value is achieved by integrating the free space position control loop and the specified contact force control law. Here, the fuzzy sliding mode control (FSMC) is proposed to design each joint position controller. When the robot hand reaches the specified working position, it is switched into a FSMC force control system based on the mapping function obtained in Section III. Then the calculated corresponding force control law was added together with the sustaining position control law to work as the driving control PWM value of each joint motor. The force control system block diagram is shown in Fig. 9. Where F_d and F_e are the desired and estimated compliance forces, respectively. The error signals for force control loop are defined as:

$$e_x = F_{xd} - F_{xe} \ , \ e_y = F_{yd} - F_{ye} \ , \ e_z = F_{zd} - F_{ze} \quad (11)$$

VI. Experimental Results

In order to achieve the specified end-effector compliance at certain working positions, the trajectory planning in Cartesian space is required for the robotic motion control. The position control loop is used to manipulate robot end-effector moving between those working positions. When the end-effector reaches the specific point, the control system is switched to force control loop. Hence, the proposed hybrid control system is switched between position control and force control loop. Here, the multi axis manipulator is planned to execute certain contacted force control at specified positions. Since the SOPC embedded system is employed to implement this robotic servo control structure, the control system cannot provide large computation ability for the model-based controller. A model-free 1D fuzzy sliding mode impedance controller is designed for a retrofitted Mitsubishi RV-M2 five DOF robotic system. In order to investigate the end-effector contacted force control performance and robustness, the following experiments were performed. The 24 seconds force control whole journey is divided into 5 steps change: initial servo motor PWM setting (0~4) sec, contact force change from initial reference to $(f_{x1} = -15N, f_{y1} = 10N, f_{z1} = -25N)$ (4~6) sec, contact force holding constant (6~14) sec, contact force change from $(f_{x1} = -15N, f_{y1} = 10N, f_{z1} = -25N)$ to $(f_{x2} = -2.5N, f_{y1} = 2.5N, f_{z1} = -45N)$ (14 ~15) sec, and contact force holding constant (14~24) sec. The sampling frequency in the experiments was set as 20 Hz. Since the sliding variable s is divided into 11 fuzzy subsets from -1 to +1 with equal interval 0.2, a parameter gs is used to regulate the sliding variables into that range. A parameter gu was used to adjust the control input.

A. Contacted Force Control at a Specified Position (450, 0, 145) mm

Firstly, the robot is moved to a specified position where the force control mapping function was established by using FSMC position controller. Then the position control closed loop is released and switched to force controller. The control input of each joint motor at the switching moment is recorded as the self-sustaining reference values. That value will be added with the force control part as the hybrid control law of each joint motor. The estimated contact force components based on hall sensors current feedback and mapping function by using FSMC force controller are shown in Fig. 10. The measured contact force components by using torque/force sensor are shown in Fig. 11 for comparison. It can be observed that the contact force tracking error in X and Y directions is less than 1 N and less than 3 N in Z direction. The experimental results by using PI control are shown in Fig. 12 for comparison. The error is bigger than FSMC control and it has big peaks appearing in the force trajectory.

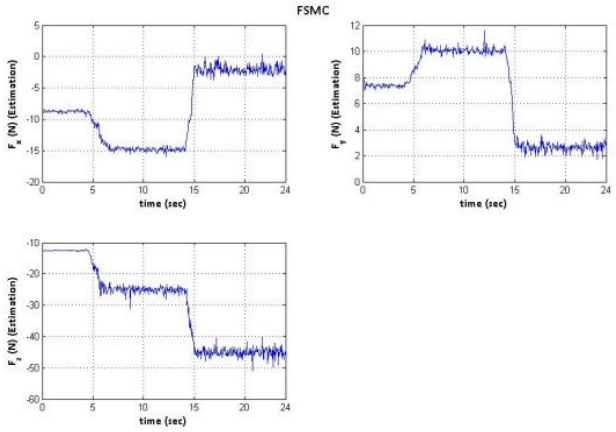

Fig. 10 Estimated contact force components based on hall sensor feedback and mapping function using FSMC controller

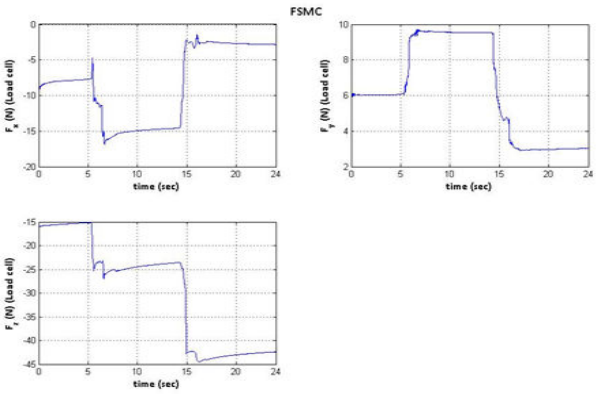

Fig. 11 Measured contact force components by using torque/force sensor

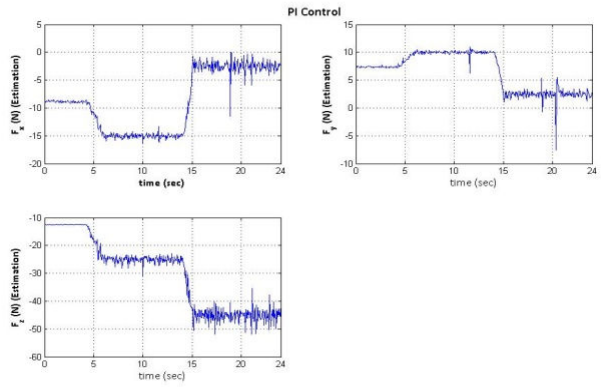

Fig. 12 Estimated contact force components based on hall sensor feedback and mapping function using PI controller

B. Contacted Force Control at a Specified Position (450, 0, 180) mm

The robot is moved to a specified working position different to the mapping function establishing point with FSMC position controller. Then the FSMC force controller is actuated to evaluate the control performance. The estimated contact force components based on hall sensors current feedback and mapping function by using FSMC force controller are shown in Fig. 13. Its real accuracy can be verified by comparing with the force sensor measuring data. If there have offset deviation between both data sets, the calibration process should be done by adding this constant offset. The reason is that mapping function is position dependent. By using this calibration process, we do not need to establish the mapping function of each working position for simplifying the implementation problem. It can be observed that the contact force mean value is accurate and the oscillation amplitude is less than 3 N in each direction. If PI controller is used, the oscillation amplitude is large than 8 N in Z direction.

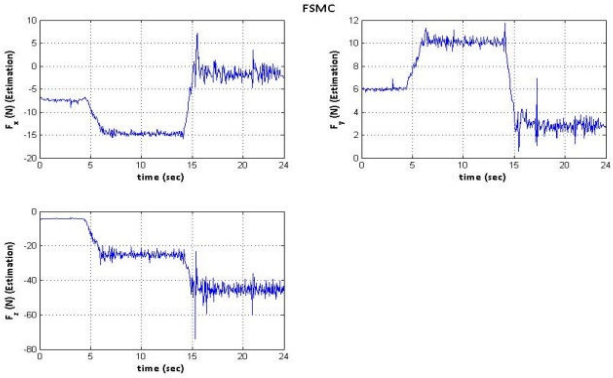

Fig. 13 Estimated contact force components based on hall sensor feedback and mapping function using FSMC controller

C. Contacted Force Control at a Specified Position (500, 0, 145) mm

The robot is moved to a specified working position different to the mapping function establishing point by using FSMC position controller. Then the FSMC force controller is actuated to evaluate the control performance. The estimated contact force components based on hall sensors current feedback and mapping function by using FSMC force controller are shown in Fig. 14. Its real accuracy can be verified by comparing with the force sensor measuring data. If there have offset deviation between both data sets, the calibration process should be done by adding this constant offset, too. The offset values for this calibration are 2, -2 and 8 N in X, Y and Z directions, respectively. The reason of this further offset calibration is that the mapping function is position dependent. It can be observed that the contact force mean value is accurate and the oscillation amplitude is less than 2 N in each direction. If PI controller is used, the oscillation amplitude is large than 10 N in Z direction.

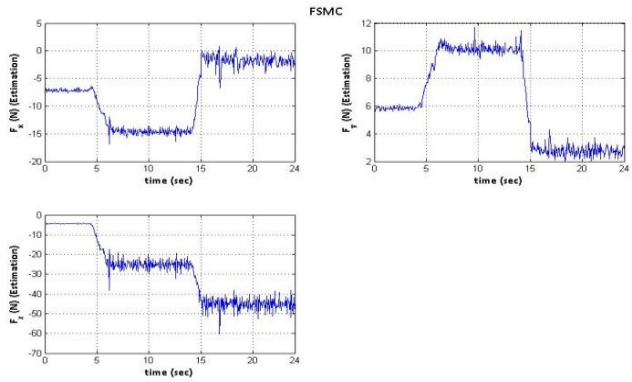

Fig. 14 Estimated contact force components based on hall sensor feedback and mapping function using FSMC controller

TABLE I
COEFFICIENTS OF 3RD POLYNOMIAL CURVE FITTING FUNCTIONS

coefficient		3rd order	2nd order	1st order	constant
J1	X	-5.5072	-1.731	3.5165	0,8797
	Y	-8.7526	-1.2718	-5.6702	-0,298
	Z	2.0898	2.9414	-0,0975	0,3861
J2	X	4.2693	-6.2801	-0,3867	1,3362
	Y	-0.4973	0.6553	-0,1581	-0,1372
	Z	26.1628	-20.2026	-3,7022	4,9282
J3	X	-4.358	-1.3075	-6,6532	-0,5689
	Y	2.0546	0.8705	-0,5635	0,0733
	Z	4.3959	3.501	3,0308	1,1644

VII. CONCLUSION

A low cost end-effector contact force control structure is constructed without expensive torque/force sensor. A nonlinear mapping function matrix between each joint motor control input and end-effector interacted force/torques vector is established at specific positions. The robot end-effector is manipulated to specified positions, then the force controller is actuated based on the hall sensor current feedback of each joint motor and this estimated mapping matrix. The position control loop self-sustaining control value is added into this force control law as the hybrid total control law. The model-free fuzzy sliding mode control (FSMC) strategy is employed to design the position and force controllers, respectively. All the hardware circuits and software control program are designed on an Altera Nios II embedded development kit to constitute an embedded system structure for a retrofitted Mitsubishi 5 DOF robot. Experimental results show that the proposed FSMC force control algorithm can achieve reasonable contact force monitoring objective based on this hardware control structure.

ACKNOWLEDGMENTS

The authors would like to thank the financial support of Taiwan National Science Council under the contract NSC-101-2221-E- 011-004-MY3.

REFERENCES

[1] N. Hogan, "Impedance control: An approach to manipulator, Parts I, II, and III," *ASME J. Dynam. Syst., Meas., Contr.*, vol. 107, pp. 1–24, Mar. 1985.
[2] Seul Jung and T. C. Hsia, "Neural network impedance force control of robot manipulators," *IEEE Trans. Ind. Electron.*, vol. 45, no. 2, pp. 451–461, 1998.
[3] S. Jung, T. C. Hsia and R. G. Bonitz, "Force tracking impedance control of robot manipulator under unknown environment," IEEE Trans. On Control System Technology, Vol. 12, No. 3, pp. 474-483, 2004.
[4] Matthew Mason, "Compliance and force control for computer controlled manipulator," IEEE Trans. On System, Man and Cybernetics, SMC-11, No. 6, pp. 418-432, 1981.
[5] M. H. Raibert and J. J. Craig, "Hybrid position and force control of robot manipulators," *ASME J. Dynam. Syst., Meas., Contr.*, vol. 102, pp. 126–133, June 1981.
[6] Shimoga B. Karunakar and Andrew A. Goldenberg, "Contact stability in model-based force control systems of robot manipulators," IEEE International Symposium on Intelligent Control, pp. 412-417, Arlington, Virginia, August, 1988.
[7] G. Ferretti, G. Magnani and P. Rocco, "Toward the implementation of hybrid position/force control in industrial robots," IEEE Trans. on Robotics and Automation, Vol. 13, No. 6, pp. 838-845, 1997.
[8] G. Ferretti, G. Magnani and P. Rocco, "Impedance control for elastic joints industrial manipulators," IEEE Trans. On Robotics and Automation, Vol. 20, No. 3, pp. 488-498, 2004.
[9] James K. Mills and Andrew A. Goldenberg, "Force and position control of manipulators during constrained motion tasks," IEEE Trans. On Robotics and Automation, Vol. 5, No. 1, pp. 30-46, 1989.
[10] L.T. Wang and C.C. Chen, "A Combined optimization Method for Solving the Inverse Kinematics Problem of Mechanical Manipulator," IEEE Trans. On Robotics and Automation Vol.7, No. 4, pp. 489-499, 1991.
[11] K. Kazerounian, "On the Numerical Inverse Kinematics of Robotic Manipulator," AMSE J of Mechanisms, Transmissions and Automation in Design, Vol.109, pp. 8-13, March 1987.
[12] Edwards Ch. And Spurgeon S. K., Sliding Mode Control – Theory and Applications, Taylor &Francis Ltd., London, Bristol, 1998.
[13] Shiuh-Jer Huang and Wei-Cheng Lin, 2003, "Adaptive Fuzzy Controller with Sliding Surface for Vehicle Suspension Control," IEEE Transactions on Fuzzy Systems, Vol. 11, No. 4, pp. 550-559.
[14] Hwang G. C. and Lin S. C., "A stability approach to fuzzy control design for nonlinear systems," Fuzzy Sets Systems, Vel 48, pp.269-278, 1992.

Shiuh-Jer Huang received the B.Sc. and M.Sc. degrees form National Taiwan University, Taipei, TAIWAN, in 1978, 1980, and the Ph.D. degree from the University of California, Los Angeles, in 1986, all in mechanical engineering department. In 1986, he joined the faculty of the Department of Mechanical Engineering, National Taiwan University of Science and Technology, Taipei, TAIWAN, where he is currently a professor. His research interests are robotic system control and applications, vibration control, Mechatronics, and vehicle active suspension control.

Sui-Hai Hsiang, and Yu-Ming Huang received the Ph.D. degree from the University of Tokyo, in 1984 and 1981, respectively, all in mechanical engineering department. In 1984, and 1982, they were joined the faculty of the Department of Mechanical Engineering, National Taiwan University of Science and Technology, Taipei, TAIWAN, where he is currently a professor. Their research interests are metal forming and extrusion, vibration control, manufacturing process and FEM application analysis.

Yu-Chi Liu is a graduate student in Department of Mechanical Engineering, National Taiwan University of Science and Technology, Taipei, Taiwan..